Effect of onsite Coulomb repulsion on thermoelectric properties of full-Heusler compounds with pseudogaps

Dat Do, Mal-Soon Lee, and S. D. Mahanti

Phys. Rev. B **84**, 125104 — Published 1 September 2011

DOI: 10.1103/PhysRevB.84.125104

Effect of on-site Coulomb repulsion on thermoelectric properties of full Heusler compounds with pseudo-gaps

Dat Do,* Mal-Soon Lee, and S. D. Mahanti
Department of Physics and Astronomy, Michigan State University, East Lansing, MI 48824, USA
(Dated: August 11, 2011)

Electronic structure calculations using local density and generalized gradient(LDA/GGA) approximations for the full Heusler compound Fe_2VAl show that it is a pseudo-gap (negative gap) system with very small density of states (DOS) at the Fermi level but rapidly rising DOS away from it, a feature that makes this compound a promising thermoelectric material. Thermopower (S) measurements in nominally pure and n-doped Fe_2VAl give indeed large values of S ($\sim$-150 μV/K at 200 K). To improve on the inadequacy of LDA/GGA in handling d-electron systems and to understand the origin of large thermopowers measured, we have carried out electronic structure calculations using GGA+U method with several values of the on-site Coulomb interaction parameter U including the ones calculated using constrained density functional theory (DFT). For the latter, we found Fe_2VAl to be a narrow band gap semiconductor with a gap of 0.55 eV. With the calculated band structures, we have studied the carrier concentration and temperature dependence of S using Boltzmann transport equation in constant relaxation time approximation for both the pseudo-gap and gapped cases. Comparison between theory and experiment suggests that neither the pseudo-gap nor the finite gap (0.55 eV) model can explain all the transport properties consistently. Therefore treatment of U beyond simple mean-field approach (done in GGA+U) and/or inclusion of defect induced changes in the host electronic structure might be important in understanding the experiments.

PACS numbers: 71.15.Mb, 71.20.-b, 72.15.Jf

I. INTRODUCTION

Thermoelectric (TE) materials have great application potential and economic impact, based on the Peltier effect for cooling and the Seebeck effect for power generation. The performance of TE materials is characterized by a dimensionless quantity called the figure of merit (ZT), $ZT = S^2\sigma T/\kappa$, where S is Seebeck coefficient or thermopower, σ is electrical conductivity, T is temperature, and κ is thermal conductivity given by the sum of the electronic (κ_e) and lattice (κ_l) contributions. There have been extensive studies to improve ZT by increasing S and σ, and decreasing κ. Among these S, σ, and κ_e are determined primarily by the electronic structure of a compound and certain characteristic features of the electronic structure are conducive to better thermoelectric properties. Thus, to improve ZT of a material it is important to understand its electronic structure. One can then use the results of the electronic structure calculations to obtain the transport coefficients using Boltzmann transport equation. However, all the transport coefficients excepting S depend sensitively on the relaxation time τ which is difficult to be determined using *ab-initio* methods. Furthermore, S has a larger impact on ZT since the later is proportional to S^2, and it is important to study S using carefully calculated electronic structure.

(Full) Heusler alloys are a class of promising thermoelectric materials. They have a stoichiometric composition with the general formula X_2YZ, where X and Y are two different transition metals and Z is a metalloid. They crystallize in a cubic structure corresponding to the space group $L2_1$. After their first discovery by Friedrich Heusler in 1903, more and more Heusler-type alloys have been found and studied extensively. Among them, Fe_2VAl based compounds came to the research community's attention in 1997 when Nishino *et al.* pointed out a possible d-electron heavy-fermion behaviour of this compound.[1] Their heat capacity measurement at low temperature (1.6-6 K) showed a linear term with a γ value of 14 mJ mol^{-1} K^{-2} from which a large electron effective mass ($10m_e$, where m_e is the free electron mass) was estimated. Photoemission spectrum showed a clear Fermi edge indicating metal-like characteristics. In contrast, by fitting the resistivity to an exponential function of E_g/T in the temperature range 400 to 800 K, Nishino *et al.* found that Fe_2VAl behaved like a semiconductor with $E_g \approx 0.1$ eV. These experimental results were quite intriguing. This dual nature was also seen in NMR experiments by Lue *et al.*[2] By measuring the T-dependence of Knight shift (K_s) and the nuclear spin relaxation time (T_1) and fitting these two quantities to functions of E_g/T, they found a band gap of 0.21-0.22 eV for K_s and 0.27 eV for T_1. Surprisingly, in addition to the activated behaviour, they also found metallic characteristics through Korringa law.[4] Using the Korringa relation, they found a finite DOS g(E_F) at the Fermi level (E_F), and estimated its V-d component to be about 1.7×10^{-2} eV^{-1} per V atom. The actual g(E_F) should be somewhat larger. Okamura *et al.*[3] using photoconductivity measurements also reported similar results for Fe_2VAl with a band gap of 0.1-0.2 eV and a finite DOS at the Fermi level. The experimental results of the band gap and the temperature range in which they were measured are summarized in Table I. Based on the activated transport measurements and the finite DOS at E_F, it was argued that Fe_2VAl was a semimetal with a pseudo-gap of 0.1$\sim$0.2 eV.

This implies that there is a small overlap between the valence band and the conduction band. This overlap gives rise to a negative band gap $E_g = E_{c,min} - E_{v,max} < 0$, where $E_{c,min}$ and $E_{v,max}$ are the extrema of the conduction and valence band, respectively. However the value of this negative band gap is not known from the experiments.

The existence of a pseudo-gap or negative band gap in the electronic structure of Fe_2VAl has been supported by several density functional (DFT) calculations within either local density approximation (LDA) or generalized gradient approximation (GGA);[5–9] a summary of these theoretical calculations is given in Table II. All the LDA/GGA calculations indicate that Fe_2VAl has a well-developed pseudo-gap with the valence band maximum (VBM) at the Γ point and the conduction band minimum (CBM) at the X point, coming mainly from the Fe-t_{2g} and V-e_g states, respectively. The negative band gap was found to be $-0.1 \sim -0.2$ eV, and there is a small but finite DOS at the Fermi level, qualitatively consistent with the Korringa law and the linear T-dependence of the heat capacity at low T. However, as we will discuss later, the calculated DOS at E_F is an order of magnitude larger than that estimated from Korringa's law and an order of magnitude smaller to explain the observed large low-T heat capacity. Nevertheless, these band structure calculations also revealed that Fe_2VAl had sharp edges in the DOS near the Fermi level which is a desirable feature for a good thermoelectric, as suggested by Mahan and Sofo.[10]

Encouraged by the sharp edges in the calculated DOS of Fe_2VAl, thermoelectric properties have been studied experimentally. In addition, several attempts have been made to increase the magnitude of S, for example by incorporating anti-site defects (increasing ratio of V/Fe)[11] or by doping at the Al site with Si, Ge, and Sn.[12–14] In the present work we will not be concerned with the V/Fe anti-site defects since they give rise to localized states near the Fermi energy and their effects on the transport properties are difficult to calculate accurately. Our focus here is to see how well one can understand the experimental data without involving the effect of defects. Experimentally it is found that nominally pure Fe_2VAl is a p-type thermoelectric (in agreement with Hall measurement.[15]) In the temperature range $T = 100 - 400$ K, S was found to be 10–50 μV/K. When Al was partially replaced by Si, Ge, or Sn[12–14], more electrons were put in the system and turned it into an n-type thermoelectric. These measurements show that the highest S (in magnitude) is about -150 μV/K, obtained for 5–6 % of Al substitution corresponding to an electron doping of 1.1–1.3$\times 10^{20}$ cm^{-3} (assuming each dopant replacing an Al donates one electron).

In spite of extensive experimental works, there is no direct spectral evidence supporting the existence of a real or pseudo gap in Fe_2VAl. From a theoretical prospective, there is also no systematic study of the relationship between the LDA/GGA electronic structure and thermoelectric properties in the pseudo-gap regime and how does theory compare with experiment. Furthermore, we know that LDA and GGA do not do well vis-à-vis band gaps in semiconductors due to the self-interaction error inherent in the LDA/GGA potential and vanishing of the discontinuity of the exchange-correlation potential as a function of the level occupation at E_F.[16] Whether there will be similar problems in pseudo-gap or zero-gap systems (when the overlap between conduction band and valence band is small) is not known. Moreover, LDA and GGA also fail to describe accurately the localized electrons in d or f states, i.e. transition metal and rare earth compounds.[16] In order to overcome the drawbacks of LDA/GGA, several methods have been developed such as: LDA+U[17], Engel-Vosko GGA,[18] modified Becke-Johnson potential,[19] hybrid functional,[20] GW,[21] etc. Recently, Bilc and Ghosez[22] used B1WC hybrid functional[23] to study Fe_2VAl and found it to be a semiconductor with a band gap of 0.34 eV. In the present work, we explore the effect of Coulomb repulsion associated with the d-electrons of Fe and V electrons Fe_2VAl using GGA+U method, which gives quite reasonable results for relatively low computational cost. This method has been found to be quite successful in several other Heusler compounds containing d-electrons such as Co_2FeSi, Co_2MnSi.[24,25]

In this paper we systematically investigate the effect of the on-site Coulomb repulsion U at both Fe and V sites on the electronic structure and thermoelectric properties of Fe_2VAl using the GGA+U approximation.[17] We first treat U as a parameter to understand how the band structure is affected by the values of U at different transition metal sites. We then calculate the values of U appropriate for this system using constrained DFT method.[26] Using the calculated band structure for these values of U we investigate the carrier concentration and temperature dependence of thermopower, look for their optimum values and compare with the experiment.

The paper is arranged as follows. In Sec. II, we briefly describe the computational procedure and give the equations for the transport coefficients within Boltzmann transport theory. We present our results and discussion in Sec. III. A brief summary is given in Sec. IV.

II. COMPUTATIONAL DETAIL

Before incorporating the effects of nonzero U, calculations of total energy (to get the optimized structure) and detailed band structure were performed using GGA with the Perdew-Burke-Ernzerhof (PBE) exchange-correlation functional,[27] and the projector-augmented wave (PAW) method[28,29] as implemented in the VASP code.[30–32] Self-consistent calculations were performed with $12 \times 12 \times 12$ Monkhorst-Pack[33] $\vec{k}$-point mesh. The energy cutoff was set to 400 eV and convergence was assumed when the total energy difference between consecutive cycles was less than

10^{-4} eV. We have checked the importance of spin orbit interaction (SOI). We found that inclusion of SOI removed the degeneracy of different bands (at symmetry points of the Brillouin Zone (BZ)) with a maximum splitting of about 0.03 eV. Thus, to reduce computational cost/time we have not included spin orbit coupling in our calculations. However for a detailed qualitative study of S, one should include the effect of SOI on the electronic structure.

The on-site Coulomb interaction was added using the approach suggested by Dudarev *et al.*[34] In this approach, referred to as the GGA+U approximation the total energy is given by:

$$E_{GGA+U} = E_{GGA} + \sum_i \frac{U_{eff,i}}{2} \sum_\sigma \left[\left(\sum_{m_1} n^\sigma_{i,m_1,m_1} \right) - \left(\sum_{m_1,m_2} n^\sigma_{i,m_1,m_2} n^\sigma_{i,m_2,m_1} \right) \right] \tag{1}$$

where E_{GGA} and E_{GGA+U} are the energies in GGA and GGA+U approximations, respectively. $U_{eff,i} = U_i - J_i$ with U_i and J_i are the Coulomb and exchange parameters for the atom at site i, m_1 and m_2 are the orbital quantum numbers ($m = -2, -1, 0, 1, 2$ for the d states) and $n^\sigma_{i,m_1,m_2}$are the matrix elements of the density operator $\hat{n}^\sigma_i$ associated with spin σ and site i in this basis. Within this approach U and J appear through the effective parameter $U_{eff} = U - J$. This simplifies our calculation since we are only interested in the combined effect of U and J.

The meaning of U was carefully discussed by Anisimov and Gunnarsson[26] and earlier works given in their references. It is defined as the energy cost for moving a d-electron between two atoms which have the same number of electrons. To obtain a numerical value of U, Anisimov and Gunnarsson[26] did supercell calculations with hopping term set to zero. The effective U was computed from the equation:

$$\begin{aligned} U_{eff} =& \epsilon_{d\uparrow}\left(\frac{n}{2}+\frac{1}{2},\frac{n}{2}\right) - \epsilon_{d\uparrow}\left(\frac{n}{2}+\frac{1}{2},\frac{n}{2}-1\right) \\ & - \epsilon_F\left(\frac{n}{2}+\frac{1}{2},\frac{n}{2}\right) + \epsilon_F\left(\frac{n}{2}+\frac{1}{2},\frac{n}{2}-1\right) \end{aligned} \tag{2}$$

where $\epsilon_{d\uparrow}(n_\uparrow, n_\downarrow)$ and $\epsilon_F(n_\uparrow, n_\downarrow)$ are respectively the spin-up d-eigenvalue and the Fermi energy for the configuration of $n_\uparrow$ up-spins and $n_\downarrow$ down-spins, n is the total number of d-electrons. Constrained DFT calculation was done using the Wien2k package[35] and following the procedure suggested by Madsen and Novák.[36] We have done $2 \times 2 \times 2$ fcc supercell calculations within PBE[27] using Γ point with a plane wave cutoff RK_{max}=7 and a Fourier expansion cutoff G_{max}=9. We found U_{eff} to be 4.0 and 1.5 eV for Fe and V, respectively. The value of U_{eff} for V is smaller than that of Fe as expected. However, the value of U_{eff} of Fe is smaller than that in Fe metal ($U_{eff} = 6.2 - 6.8$ eV)[26] and in oxide ($U_{eff} = 4.8 - 7.4$ eV),[36] suggesting strong screening effect in Fe_2VAl obtained within this approximation.

We first investigate the effect of Coulomb repulsion with various values of U on Fe and V sites separately to understand how different bands are affected by U. For this purpose we consider three situations for each atom: weak (U_{eff} =1 eV), intermediate (U_{eff} =2 eV), and strong (U_{eff} =4 eV) repulsion limits (comparing to typical d bandwidth of 1.5–2 eV). We then carried out GGA+U calculation with U values obtained using the constrained DFT method. In the rest of the paper we will omit the suffix "eff" from U_{eff}.

Thermopower S was calculated using Boltzmann transport equation in constant relaxation time and rigid band approximations.[37] Since Fe_2VAl is a cubic system, its transport tensors are diagonal and all the diagonal elements are the same. Electrical conductivity σ and thermopower (Seebeck coefficient) S are given by

$$\sigma = e^2 \int_{-\infty}^{+\infty} d\epsilon \left(-\frac{\partial f_0}{\partial \epsilon}\right) \Sigma(\epsilon), \tag{3}$$

$$S = \frac{e}{T\sigma} \int_{-\infty}^{+\infty} d\epsilon \left(-\frac{\partial f_0}{\partial \epsilon}\right) \Sigma(\epsilon)(\epsilon - \mu), \tag{4}$$

where μ is the chemical potential, e is the electron charge, f_0 is the Fermi-Dirac distribution function, and $\Sigma(\epsilon)$, called the transport distribution function, is given by

$$\Sigma(\epsilon) = \sum_{n,\vec{k}} \nu_x(n,\vec{k})^2 \tau(n,\vec{k}) \delta(\epsilon - \epsilon(n,\vec{k})). \tag{5}$$

In Eqn. (5), n is the band index and the summation is over the first Brillouin zone (BZ), $\nu_x(n,\vec{k})$ is the carrier velocity of an electron in state $(n,\vec{k})$ along the x direction (cubic axis), and $\tau(n,\vec{k})$ is the relaxation time. In our calculation

we have assumed $\tau(n,\vec{k})$ to be constant. For calculations of σ and S, we first obtained the energy dispersion with Monkhorst-Pack mesh of $41\times41\times41$ $\vec{k}$-points, and transport coefficients were calculated from the resulting eigenvalues using equations (3) and (4) with constant τ, employing the Boltztrap code developed by Madsen and Singh.[37] As mentioned earlier, we will discuss only the thermopower S.

III. RESULTS AND DISCUSSION

A. Electronic structure

In Fig. 1 (left panel) we show the energy bands along different symmetry directions of the first BZ together with Fe- and V-d characters. On the right panel we give the DOS which clearly shows a pseudo-gap structure near E_F. The zero of energy has been chosen to be the Fermi level. Our GGA band structure results agree with the previous GGA calculations of other groups.[5–9] Fe_2VAl has a negative band gap of $E_g = -0.17$ eV. Certain general features of the band structure are the following: It has a deep and rather broad Al s-band from -10 to -6 eV. The bands from -5 to 2 eV result from the hybridization of Fe and V d-orbitals with a small admixture of Al p-orbitals (only Fe-d and V-d characters are shown in Fig. 1). The pseudo-gap is formed by a nondegenerate V-e_g band minimum at the X point and a three-fold degenerate Fe-t_{2g} band at the Γ point. Near 0.3 eV there is a very narrow band originating from Fe-e_g states which gives rise to a sharp edge in the conduction band DOS. These Fe- and V-d bands are important features which are relevant to the low energy physics in general and the thermoelectric properties in particular. The band structure of Fe_2VAl near the Fermi-level shows that there are three-fold degenerate hole pockets centered around the Γ point with nearly same effective mass and a nondegenerate electron pocket centered around the X point. Since there are three inequivalent X points in the BZ this compensates for the 3-fold degeneracy of valence band when one compares the contributions from the valence band holes and conduction band electrons to the thermopower. The calculated DOS at the Fermi energy for the undoped system is 0.27 eV^{-1}/f.u. This gives a γ value for the linear heat capacity of 0.63 mJ mol^{-1} K^{-2}, nearly the same as 0.69 mJ mol^{-1} K^{-2} reported by Guo *et al.*[8] The small difference between the two theoretical values is due to the different lattice constants and different methods used. However, both these values are order of magnitude smaller than the experimentally measured low-T γ value of 14 mJ mol^{-1} K^{-2}.[1]

As seen in Fig. 1 (right panel), there is a rapid rise in the DOS near 0.3 eV (in the conduction band) and a similar but less rapid rise at -0.2 eV (in the valence bands). As we will discuss later, one obtains large values of S (magnitude) when Fe_2VAl is heavily doped, either n-type or p-type, because the chemical potential approaches these rapidly increasing parts of the DOS.

When the on-site Coulomb repulsion U is turned on, as one would expect (see reference 17) the occupied states are pushed down in energy whereas the unoccupied states are pushed up. This is clearly seen in Figs. 2 and 3. In order to see how different bands change due to the on site Coulomb repulsion, we plot the band structure in the absolute scale focusing on the bands near the Fermi level in the range from -11 to -7 eV. Fig. 2 shows the band structures with U_{Fe} =0,1, 2, and 4 eV at the Fe site only. In this case V bands are relatively unaffected while the unoccupied Fe-e_g bands are pushed up and the occupied Fe-t_{2g} bands are pushed down. For a quantitative measure of the effect of U_{Fe}, we define a quantity $\Delta_{e_g,t_{2g}}$ which is the splitting between the Fe-e_g conduction band and the Fe-t_{2g} topmost valence band at the Γ point. The value of $\Delta_{e_g,t_{2g}}$ changes by 0.22, 0.48 and 1.18 eV for U_{Fe}=1, 2, and 4 eV, respectively. As expected, the larger the value of U_{Fe}, the larger is the change in the energy difference. However, the changes in the energies are about 22$\sim$30 % of the values of the parameter U_{Fe}. This is due to the hybridization of Fe-d, V-d and some Al-p orbitals. In the weak repulsion regime, the parameter U_{Fe} has very small effect on the band gap. In the intermediate and strong repulsion cases the effects are significant. The relative shift of the bands results in changing the pseudo gap to a real gap. For $U_{Fe} = 1$ eV the pseudo-gap remains while the values of the band gap are 0.002 eV and 0.27 eV corresponding to $U_{Fe} = 2$ eV and 4 eV, respectively.

Looking more carefully at the changes in the band structures (see Fig. 2), one can point out an interesting change in Fe-t_{2g} bands at the X point. In the absence of U_{Fe}, the t_{2g} bands of Fe splits into two levels, where a nondegenerate band is located at $\approx$0.15 eV above the two-fold degenerate one. We note here that the nondegenerate band consists of Fe-t_{2g} only while the two-fold degenerate band shows strong hybridization, with a small contribution of Fe-t_{2g} and large contribution of p-like plane-wave states. On the other hand, at the Γ point, the VBM is 3-fold degenerate coming from hybridization of Fe- and V-t_{2g} orbitals. In the presence of U_{Fe}, the bands without hybridization are strongly affected by U_{Fe}, whereas the bands with stronger hybridization, specially when p states are involved, are not affected much by U_{Fe}. This results in the change in the ordering of these levels (at X and Γ) when U_{Fe}=4 eV. The nondegenerate band is pushed down more strongly than the two-fold degenerate one. As a consequence, when U_{Fe}=4 eV, reversed ordering of these levels is observed at the X point, i.e. the two-fold degenerate Fe-t_{2g} band becomes the highest occupied band. This makes the system a direct band gap semiconductor and also brings more hole pockets into the system even with small doping levels. This would make Fe_2VAl a better p-type thermoelectric

(which will be discussed in detail later in this paper). Similar effect is also seen in Fe-e_g conduction bands. Without U_{Fe}, at the X point, the second and fourth lowest-energy bands have pure Fe-e_g character while the third one is a hybridized band of Fe-e_g and V-t_{2g}. By turning on the Fe-site Coulomb repulsion, the energy difference between the second and fourth bands remain nearly the same, whereas that between the second and third bands is decreased.

Similar band shifting is seen when we turn on the Coulomb repulsion at the V site only: The Fe bands remain nearly unchanged while the V-e_g bands, since they are mainly unoccupied, are shifted upwards (shown in Fig. 3). There is however a difference in the way V d-bands react when we include U effect on the V site. The V-e_g bands, most of which lies above the Fermi level, is affected strongly by U_V since it is predominantly of V-e_g character. The energy of this band is changed about 13–20 % of the U_V value. On the other hand, the occupied bands which hybridize with Fe-t_{2g} are shifted by less than 1 % of the U_V value (Note that U_{Fe}=0). In the case when one considers U_V at the V site only, even a weak repulsion causes a significant change in the band gap. For U_V=1 eV, Fe_2VAl becomes an almost zero-gap system; for U_V=2 eV there is a real gap of 0.21 eV; when U_V=4 eV the V-e_g band is pushed up so much that the flat Fe-e_g band becomes the lowest conduction band and the gap is now 0.32 eV.

When we turn on U at both Fe and V sites the net effect appears to be roughly a combination of individual Fe and V effects. For the U values obtained from constrained DFT as described in Sec. II (U_{Fe} =4 eV and U_V =2 eV), the calculated band structure is shown in Fig. 4(b). A band gap of 0.55 eV is obtained and it is both direct and indirect since the highest occupied states at the Γ and the X points are nearly degenerate (as discussed in the case U_{Fe} =4 eV above).

As mentioned in Sec. I, several improvements beyond LDA/GGA have been done to take better account of localized d-electron systems, including improved GGA by Engel and Vosko[18], hybrid functional: PBE0,[38] and B1WC[23]. Recently Tran and Blaha[19] proposed a new semi-local potential model called modified Becke-Johnson (mBJ) in which they include the kinetic energy density term and fix the parameters by applying to a wide range well known systems and fitting the obtained band gaps to the experimental values. This new potential is claimed to give good band gap values which agree well with those obtained using the GW method.[21] For comparison with our GGA+U calculation, we have also done calculations using mBJ as well as the other methods. The summary of methods and corresponding band gaps are given in Table III and the band structures obtained from some of these methods are shown in Fig. 4. Here GGA and GGA+U calculations were done with VASP[30–32], while the other calculations were done using Wien2k[35]. PBE0 and B1WC are hybrid functional where there is a fraction α contribution of none local Hartree-Fock exchange to the total exchange-correlation potential, the other fraction $1-\alpha$ being local. We found that both PBE0 and B1WC with $\alpha = 0.25$ give quite large band gaps, 0.58 and 0.62 eV, which are very close to our GGA+U result. Reducing the value of α to 0.16 in B1WC method results in the band gap of 0.34 eV. These values are, however, larger than that obtained from mBJ method which gives 0.22 eV (in reasonable agreement with experimental band gap). It is worthwhile to mention that mBJ method, among all the methods we have tried, gives the energy level ordering at the X point very similar to that of seen in the GGA+U calculation. However the change in the band structure seen in mBJ (compare to GGA calculation) is not as large as that seen in GGA+U. Hence the top of the valence band is still at the Γ point and the band gap is indirect in the mBJ band structure.

If mBJ method indeed gives the right band gap for Fe_2VAl and this compound is an intrinsic narrow band gap semiconductor then the large gap (0.55 eV) obtained from GGA+U calculation suggests that the constrained DFT method proposed by Anisimov and Gunnaarsson overestimates the value of U, at least in these ternary compounds with small band gaps. In their method, Anisimov and Gunnarsson only considered the screening from s and p electrons and neglected the effect of d electrons themselves. This might underestimate the screening effect on U because small band gap in this system involves excitations of d-electrons. Suppression of these excitations will tend to give large U values. Having noted this shortcoming of the present U calculations we have tried smaller values of U. We found that mBJ result could be reproduced by GGA+U with U_{Fe}=3 eV and U_V=1 eV. The similarity in the results obtained from mBJ and GGA+U calculation may be worth a further study.

B. Thermoelectric properties

Thermopower S was calculated using Eqns. (3) and (4) for different doping levels (different concentrations) and for different temperatures (T) in the range 100–700 K.

1. GGA calculation

First let us consider the case when U=0 eV (GGA calculation). This corresponds to the negative gap or pseudo-gap picture in which Fe_2VAl is a semi-metal with a small but finite DOS at E_F. In the absence of any doping the electron concentration (n_e) and hole concentration (n_h) are the same. We define the carrier concentration as

$n = \frac{1}{V}(N - \int_{-\infty}^{+\infty} D(\epsilon) f_0 d\epsilon)$, where N is the total number of electrons in the system, V is the volume, $D(\epsilon)$ is the density of states and $f_0(\epsilon)$ is the Fermi-Dirac distribution function. The sign of n corresponds to the sign of the charge of the carriers. $n_e = -n$ when n is negative and $n_h = n$ when n is positive. With this definition, carrier concentration is equivalent to the doping level in the experiment. We change n by changing the chemical potential and see how S changes with n, and T. Fig. 5 shows thermopower (S) and chemical potential (μ) as a function of n for two different temperatures, 300 K and 700 K. Although the magnitude of S increases with T, the higher T the smoother is the variation of S with n, caused by enhanced thermal broadening of the Fermi distribution function (see Eqn. 4). The magnitude of S has two peaks for n-type doping, the first one at $n_e \approx 5.1 \times 10^{20}$ cm^{-3} and the second at $n_e \approx 5.0 \times 10^{21}$ cm^{-3}. For p-type doping there is only one peak at and $n_h \approx 2.3 \times 10^{21}$ cm^{-3}. These three concentrations correspond to the chemical potential of 0.13, 0.43, and -0.18 eV, respectively.

We can understand these peaks in magnitude of S by analysing the band structure of Fe_2VAl. Let's first understand the n-type thermopower as a function of n. Without doping the chemical potential lies in the overlap region between conduction band and valence band (see Fig. 4-(a)). In this region the hole and electron contribution in S cancels each other resulting in very small magnitude of S following the equation $S = \frac{S_e\sigma_e + S_h\sigma_h}{\sigma_e + \sigma_h}$, where S_e, σ_e and S_h, σ_h are thermopowers and electrical conductivities associated with the electrons and holes, respectively. When n_e increase, the chemical potential increases (moves away from the Fermi level) and eventually gets out of the overlap region at 0.13 eV. As a result, the hole-electron cancellation is suppressed. The suppression of hole-electron cancellation gives rise to the first peak in the n-type S. The second peak in n-type S is obtained when n is high enough for chemical potential to reach the flat band of Fe at 0.43 eV. At this point the magnitude of S gets a high value due to the rapid change in DOS.

Similarly, one can see that the peak in p-type S is due to both suppression of hole-electron cancellation effect and the rapid rise in DOS near -0.18 eV. The coincidence of two events: getting out of the overlap region and reaching the rapid rise in DOS is the reason why there is only one peak in the magnitude of p-type S.

It appears from these results that if the band structure of Fe_2VAl is adequately described by LDA or GGA, i.e. it is a pseudo-gap system, then to have large thermopower values one has to go to rather high doping levels when the cancellation effects are nearly absent. However, the carrier concentrations should not be so large that Pauli suppression for degenerate carriers start to reduces $|S|$.

Now let us look at thermopower as a function of temperature. Fig. 6 plots S versus T for several carrier concentrations. We will consider n- and p-type dopings separately.

n-type doping: In the temperature range 100–700 K, S has the highest value (magnitude) for $n_e \approx 4 - 6 \times 10^{21}$ cm^{-3}. The magnitude of S increases with T, but the increase is rapid at low T and then slows down at high T. At high T, large number of electron and hole excitations start to dominate resulting in a cancellation and reduction in S. This results in the flattening and eventual decrease in the magnitude of S with increasing T (>700 K). This electron-hole cancellation is also the reason for small magnitude of S values seen for small n.

p-type doping: One sees behaviour similar to the n-type doping. Again S increases with T and has small values for low concentrations due to electron-hole cancellation. S is largest (100 μV/K) for $n_h \approx 2{\times}10^{21}$ cm^{-3}. Interestingly, GGA calculation shows that Fe_2VAl is a slightly better p-type thermoelectric than n-type. For example, at 700 K, the highest value of the magnitude of S is 110 μV/K for p-doping and only 80 μV/K for n-doping, about 30 % smaller. To understand this difference we look at the band structure. The electron pockets center around the X points and are non-degenerate (ignoring spin degeneracy), whereas the hole pockets center around the Γ point but are three-fold degenerate. Since there are three inequivalent X points in the BZ and only one Γ point, the difference in the S value cannot be ascribed to the band degeneracy. We believe it is due to the difference in the effective masses of electrons and holes. The Fe dominated holes have larger effective mass and lead to larger S values. This property of the Fe_2VAl is different from the other class of Heusler compound ZrNiSn.[39] In the latter compounds the electron pockets centered around the X points are heavier than the hole pockets centered around the Γ point. Consequently the magnitude of the thermopower is larger for the electrons in ZrNiSn.[39]

2. *GGA+U calculation : the effect of finite band gap*

As we have discussed earlier the effect of incorporating U is to decrease the overlap between the valence and the conduction bands and eventually open up the gap. For U_{Fe}=4 eV and U_V=1.5 eV (values calculated using constrained DFT), the band gap is 0.55 eV. For the calculation of the transport coefficients we choose the zero of energy at the middle of the gap. In Fig. 7 we give the results of S as a function of T for different values of the concentration. The T-dependence of S for the case of real gap is much simpler compared to the pseudo-gap case. Since there is very little electron-hole cancellation, S follows the Pizarenko relation, i.e. the magnitude of S increase with decreasing carrier concentration. Thus, doping makes S worse. And for the same reason S does not saturate up to 700 K as the thermal excitations of electrons and holes are suppressed due to the large band gap.

As mentioned above, in the present of U, valence band maxima near Γ and X points become nearly degenerate. Since more hole pockets contribute to transport (both at the Γ and X points) (see Fig. 4(b)) we found that opening up of the gap by U leads to a better p-type thermoelectric. The value of S for the p-type at concentration of 5×10^{19} cm^{-3} at 700 K is about 3/2 times larger than that for the n-type at the same carrier concentration and temperature.

C. Comparison with experiment and other theoretical results

For comparison between theory and experiment we will use the experimental results on $Fe_2VAl_{1-x}Ge_x$ by Nishino *et al.*[12] and $Fe_2VAl_{1-x}Si_x$ by Skoug *et al.*[14] for x values in the range 0.0–0.2. Although these two systems are similar and show qualitatively similar behaviours, there are quantitative differences which might help us in testing our theoretical calculations, particularly the adequacy of the pseudo-gap (or semimetal) picture.

Let us first look at the nominally undoped system (x=0). Both experiments show p-type behaviour in the temperature range 100–400 K. S of nominally undoped system increases slightly with T and saturates between 300–400 K. The values of S at 300 K, however, differ by nearly a factor of 2 between the two measurements (25 and 50 μV/K obtained by Nishino *et al.* and by Skoug *et al.* respectively). One can argue that this difference can be due to the difference in the hole concentrations and the small values of S can be understood within the pseudo-gap model when the hole concentration lies between 10^{20}–10^{21} cm^{-3}, because in this model, the electron–hole cancellation effect makes S to be not only small in magnitude but also a weak function of carrier concentration over a wide range. (see Fig. 8). In contrast, for a finite gap case (especially for a large gap 0.55 eV as obtained in the GGA+U calculation) one can not understand the peak in S because S follows the Pizarenko relation and changes rapidly as the function of carrier concentration (see Fig. 8). From Hall measurement done by Nishino *et al.* [15], the hole concentration for the nominally undoped sample is found to be $\approx 5\times10^{20}$ cm^{-3}. For this concentration the GGA+U band structure gives $S\approx 140\mu V/K$ at 300 K, which is about two times larger than the experimental values (25 and 50 μV/K), while GGA band structure gives $S\approx 30\mu V/K$ in quite good agreement with experiment. This result would then favour the pseudo-gap or semimetal picture. Physically, this means that when the hole concentration is not too large, small S values can be obtained near 300 K only when there is significant electron-hole cancellation.

When one replaces Al by Ge, Si, or Sn, the dopants give an extra electron/dopant to the network and when $x > 0.03$, the alloys show n-type behavior. One significant feature in the n-type compounds studied by both Nishino and Skoug's groups is that for the optimum doping (x ≈0.05–0.06), S shows a minimum between 200–300 K and the value of S near the minimum is about -150 μV/K[12,14]. For larger x (presumably for larger carrier concentration), the minimum moves towards higher T.

Studying S as the function of T corresponding to the pseudo-gap case (U=0) (Fig. 6), we found that that for the entire range of electron concentration $n_e \approx 5\times10^{19} - 10^{22}$ cm^{-3}, there is no discernible minimum in S at temperature lower than 500 K and also the magnitude of the S values are less than 60 μV/K (two times smaller than the experimental values) in the temperature range 100–700 K. Both these observations are in disagreement with experiments. So neither the pseudo-gap model nor the model with large band gap (∼0.55 eV) can explain the observed minimum in S at $T\sim 300K$ and its magnitude.

In an attempt to see if a finite gap picture could explain the experimental data we have tried using smaller values of U than that obtained from the constrained DFT calculation. We found that with very small U (≈1 eV) (and almost zero band gap,$E_g\approx 0.07eV$) we could qualitatively reproduce the experimental data of S for n-type system, particularly the minimum at ∼ 300 K (see Fig. 9). However in order to get such an agreement with experiment we had to use values of $n\approx 5\times10^{19}$ cm^{-3} which is about one order of magnitude smaller than that obtained from the Hall measurement.[12] For the p-type (nominally undoped) system with hole concentration of 5×10^{20} cm^{-3} (obtained from Hall measurement[12]) we found that the magnitude of S is roughly of the order of the experiment done by Skoug *et al.* However, S does not saturate in the range 0–700 K.

From the above analysis, we see that it is difficult to understand the experimental data for both the nominally undoped and n-doped cases using either the pseudo-gap or the real gap model. This conclusion agrees with the work of Bilc and Ghosez[22]who used B1WC hybrid functional method[23] and found a band gap of about 0.34 eV which lies between our value of 0.55 eV and the experimental value of about 0.2 eV. With this value of band gap they could not reproduce the experimental data. So just scaling the gap to a small value cannot explain the n,T-dependence of S. In order to understand the difference between experiment and theory, one has to overcome several weaknesses of the present calculations.

First, the effect of inter-site Coulomb repulsion between d-electrons at neighbouring V- and Fe-sites has not been included within the present GGA+U approach. Also, GGA+U is essentially a mean-field approximation, and does not include electron-hole excitonic correlations which may alter the electronic states near the Fermi energy in the pseudo-gap or small gap regime. Second, we have used a rigid band model to calculate S. It is possible that the dopants distort the electronic structure near the Fermi energy and hence the rigid band model is not valid any more.[40]

Third, there may be defects (Fe-V antisite defects, vacancies, and interstitials) which alter the states near the Fermi energy, giving rise to not only new (and perhaps smaller than the band gap) excitation energy scales but also to localized states that act as carrier traps.

IV. SUMMARY

In this paper we have discussed how the band structure of Fe_2VAl changes when one takes into consideration the effect of intra-site Coulomb repulsion between d-electrons at the Fe and V sites beyond GGA using GGA+U approximation. In Heusler compounds, which contain two different types of transition metal atoms, the effect of U on the band gap depends sensitively on which one of the two transition metal sites one is dealing with. For example, even small values of U_V ($\sim$1 eV) at the V site can open up the gap because the lowest conduction band is predominantly V d-character and gets pushed upward in energy strongly by U_V. In contrast, small values of U_{Fe} ($\sim$1 eV) at the Fe site do not open up the gap, rather changes the band structure slightly. This is because the top of the valence band is strongly hybridized and is shifted downwards in energy only slightly. Thus one needs a larger value of U_{Fe} ($\sim$2 eV) at the Fe site to open the band gap when $U_V = 0$.

The values of U calculated using constrained density functional theory (U_{Fe}=4 eV for Fe and U_V=1.5 eV for V) are much smaller than the atomic values of U ($\sim$20 eV) indicating a strong screening effect. This is not surprising and is seen in many transition metal compounds. What surprising is that the values we have calculated for Fe is smaller than that one finds in Fe metal ($\sim$6 eV) since the screening should be stronger in the metal.

Using the values U_{Fe}=4.0 eV and U_V=1.5 eV we find that the gap is 0.55 eV, considerably larger than that obtained from transport measurements and NMR ($e_g \approx 0.2\ eV$). In this case, S shows characteristics of usual narrow band-gap semiconductor. Both GGA and GGA+U calculations suggest that Fe_2VAl is a better p-type thermoelectric either due to larger hole effective mass (in GGA) or due to large degeneracy (in GGA+U).

Our calculations, however, point out that the present models (both pseudo and real intrinsic gap cases), cannot explain all the experimental data on S consistently for both n- and p-doped cases. Band structure calculated using hybrid functional and modified Becke-Johnson potential tend to give small band gaps (0.34 eV and 0.22 eV). But these values are still too large to explain the thermopower data. Several limitations of the present models, such as the electron-hole (excitonic) correlation effects, defect induced changes in band structure, etc. , were pointed out and further work is in progress.

Acknowledgments

The authors would like to thank the referees for valuable suggestions. We also would like to thank Dr. Donald Morelli for useful discussions on experimental perspective.

This material work was supported by the Center for Revolutionary Materials for Solid State Energy Conversion, an Energy Frontier Research Center funded by the U.S. Department of Energy, Office of Science, Office of Basic Energy Sciences under Award Number DE-SC0001054.

* dodat@msu.edu; http://www.msu.edu/~dodat

[1] Y. Nishino, M. Kato, S. Asano, K. Soda, M. Hayasaki, and U. Mizutani, Phys. Rev. Lett. **79**, 1909 (1997).
[2] C.-S. Lue and J. H. Ross, Phys. Rev. B **58**, 9763 (1998).
[3] H. Okamura, J. Kawahara, T. Nanba, S. Kimura, K. Soda, U. Mizutani, Y. Nishino, M. Kato, I. Shimoyama, H. Miura, et al., Phys. Rev. Lett. **84**, 3674 (2000).
[4] J. Korringa, Physica **16**, 601 (1950).
[5] D. J. Singh and I. I. Mazin, Phys. Rev. B **57**, 14352 (1998).
[6] M. Weinert and R. E. Watson, Phys. Rev. B **58**, 9732 (1998).
[7] R. Weht and W. E. Pickett, Phys. Rev. B **58**, 6855 (1998).
[8] G. Y. Guo, G. A. Botton, and Y. Nishino, J. Phys.: Condens. Matter **10**, L119 (1998).
[9] M. Kumar, T. Nautiyal, and S. Auluck, Journal of Physics: Condensed Matter **21**, 446001 (2009).
[10] G. D. Mahan and G. O. Sofo, in Proc. Natl. Acad. Sci. (1996), vol. 93, p. 7435.
[11] C. S. Lue and Y.-K. Kuo, Phys. Rev. B **66**, 085121 (2002).
[12] Y. Nishino, S. Deguchi, and U. Mizutani, Phys. Rev. B **74**, 115115 (2006).
[13] M. Vasundhara, V. Srinivas, and V. V. Rao, Phys. Rev. B **77**, 224415 (2008).
[14] E. J. Skoug, C. Zhou, Y. Pei, and D. T. Morelli, Jr. Electronic. Matter **38**, 1221 (2009).
[15] Y. Nishino, Intermetallics **8**, 1233 (2000).
[16] R. M. Nieminen, Topics in Applied Physics: Theory of defects in semiconductors (Springer, 2006), vol. 104, pp. 36–40.
[17] V. I. Anisimov, F. Aryasetiawan, and A. I. Lichtenstein, Journal of Physics: Condensed Matter **9**, 767 (1997).
[18] E. Engel and S. H. Vosko, Phys. Rev. B **47**, 13164 (1993).
[19] F. Tran and P. Blaha, Phys. Rev. Lett. **102**, 226401 (2009).
[20] A. D. Becke, The Journal of Chemical Physics **98**, 1372 (1993), URL http://link.aip.org/link/?JCP/98/1372/1.
[21] L. Hedin, Phys. Rev. **139**, A796 (1965).
[22] D. I. Bilc and P. Ghosez, Phys. Rev. B **83**, 205204 (2011).
[23] D. I. Bilc, R. Orlando, R. Shaltaf, G.-M. Rignanese, J. Íñiguez, and P. Ghosez, Phys. Rev. B **77**, 165107 (2008).
[24] H. C. Kandpal, G. H. Fecher, C. Felser, and G. Schönhense, Phys. Rev. B **73**, 094422 (2006).
[25] B. Balke, G. H. Fecher, H. C. Kandpal, C. Felser, K. Kobayashi, E. Ikenaga, J.-J. Kim, and S. Ueda, Phys. Rev. B **74**, 104405 (2006).
[26] V. I. Anisimov and O. Gunnarsson, Phys. Rev. B **43**, 7570 (1991).
[27] J. P. Perdew, K. Burke, and M. Ernzerhof, Phys. Rev. Lett. **77**, 3865 (1996).
[28] P. E. Blöchl, Phys. Rev. B **50**, 17953 (1994).
[29] G. Kresse and D. Joubert, Phys. Rev. B **59**, 1758 (1999).
[30] G. Kresse and J. Hafner, Phys. Rev. B **47**, 558 (1993).
[31] G. Kresse and J. Furthmüller, Computational Materials Science **6**, 15 (1996).
[32] G. Kresse and J. Furthmüller, Phys. Rev. B **54**, 11169 (1996).
[33] H. J. Monkhorst and J. D. Pack, Phys. Rev. B **13**, 5188 (1976).
[34] S. L. Dudarev, G. A. Botton, S. Y. Savrasov, C. J. Humphreys, and A. P. Sutton, Phys. Rev. B **57**, 1505 (1998).
[35] K. Schwarz and P. Blaha, Computational Materials Science **28**, 259 (2003), ISSN 0927-0256, proceedings of the Symposium on Software Development for Process and Materials Design, URL http://www.sciencedirect.com/science/article/pii/S0927025603001125.
[36] G. K. H. Madsen and P. Novák, Europhys. Lett. **69**, 777 (2005).
[37] G. K. Madsen and D. J. Singh, Computer Physics Communications **175**, 67 (2006).
[38] C. Adamo and V. Barone, The Journal of Chemical Physics **110**, 6158 (1999), URL http://link.aip.org/link/?JCP/110/6158/1.
[39] P. Larson, S. D. Mahanti, S. Sportouch, and M. G. Kanatzidis, Phys. Rev. B **59**, 15660 (1999).
[40] M.-S. Lee and S. D. Mahanti, to be published.

Figures

FIG. 1: (Color online) Band structure of Fe_2VAl showing d-characters of Fe and V (left); and DOS (right). E_F denotes the Fermi level set to be zero. The size of the symbols represents the strength of orbital characters.

FIG. 2: (Color online) Band structure of Fe_2VAl in absolute scale for U_{Fe} of (a) 0 eV, (b) 1 eV, (c) 2 eV and (d) 4 eV. The Fe-e_g and Fe-t_{2g} bands are pointed out by arrows.

FIG. 3: (Color online) Band structure of Fe_2VAl in absolute scale for U_V of (a) 0 eV, (b) 1 eV, (c) 2 eV and (d) 4 eV.The V-e_g bands are pointed out by an arrow.

FIG. 4: (Color online) Band structure of Fe_2VAl obtained in different methods: (a) GGA-PBE[27], (b) GGA+U[17], (c) mBJ[19] and (d) PBE0[38].

FIG. 5: (Color online) Thermopower (S) and chemical potential (μ) versus carrier concentration (n_e, n_h) in the absence of U (the pseudo-gap case) for n- and p-type doping. The Fermi level is chosen to be 0.

FIG. 6: (Color online) S as functions of temperature obtained using the GGA band structure (U=0 eV, the pseudo-gap case) at different concentrations: for n-type (closed symbols) and p-type (open symbols) doping.

FIG. 7: (Color online) S as functions of T for GGA+U calculation (U_Fe=4 eV and U_V=1 eV) at different concentration: for n-type (closed symbols) and p-type (open symbols) doping.

FIG. 8: (Color online) Calculated p-type S as a function of n for the cases of: pseudo-gap (GGA calculation) (solid line) and gapped (GGA+U calculation), E_g=0.55 eV, (dashed line) at 300 K.

FIG. 9: (Color online) Experimental thermopower obtained by doping Si on Al site (symbols) (done by Skoug *et al.* [14]) and theoretical curve (lines) with U=1 eV ($E_g = 0.07\ eV$). (carrier concentrations are given in unit of cm^{-3})

Tables

TABLE I: Summary of experimental studies of energy gap in Fe_2VAl

Group - year	Measured quantity	E_g (eV)
Nishino *et al.* - 1997[a]	Resistivity (400–800 K)	0.1
Lue *et al.* - 1998[b]	NMR (250–550K)	
	• Knight shifts (K_s)	0.21–0.22
	• Spin relaxation rate (T_1)	0.27
Okamura *et al.* - 2000[c]	Photo-conductivity (9–295K)	0.1 - 0.2

[a]Reference 1
[b]Reference 2
[c]Reference 3

TABLE II: Summary of previous theoretical studies on Fe_2VAl electronic structure

Group - Year	Method	a(Å)	E_g (eV)	g(E_F) ($eV^{-1}/f.u.$)
Singh & Mazin - 1998[a]	LSDA, LAPW (LMTO)	5.76	-0.2	0.3
Weinert & Watson - 1998[b]	LDA, (FLASTO)		-0.2	–
Weht & Pickett - 1998[c]	GGA, PBE	5.76	-0.2∼-0.1	0.1
Guo *et al.* - 1998[d]	LSDA	5.68	-0.2	0.54
Kumar *et al.* - 2009[e]	GGA, PBE	5.712	–	0.19

[a]Reference 5
[b]Reference 6
[c]Reference 7
[d]Reference 8
[e]Reference 9

TABLE III: Summary of Fe_2VAl band gap using different methods

Method	Parameter	Band gap (eV)
GGA–PBE[a]	–	-0.17
GGA–EV[b]	–	-0.06
GGA+U[c]	$U_{Fe} = 4$ eV, $U_V = 1.5$ eV	0.55
mBJ[d]	–	0.22
PBE0[e]	$\alpha = 0.25$	0.58
B1WC[f]	$\alpha = 0.16$[g]	0.34
	$\alpha = 0.25$	0.62

[a]Reference 27
[b]Engel-Vosko GGA[18]
[c]Reference 17
[d]Reference 19
[e]Reference 38
[f]Reference 23
[g]The value used by Bilc *et al.* [22]

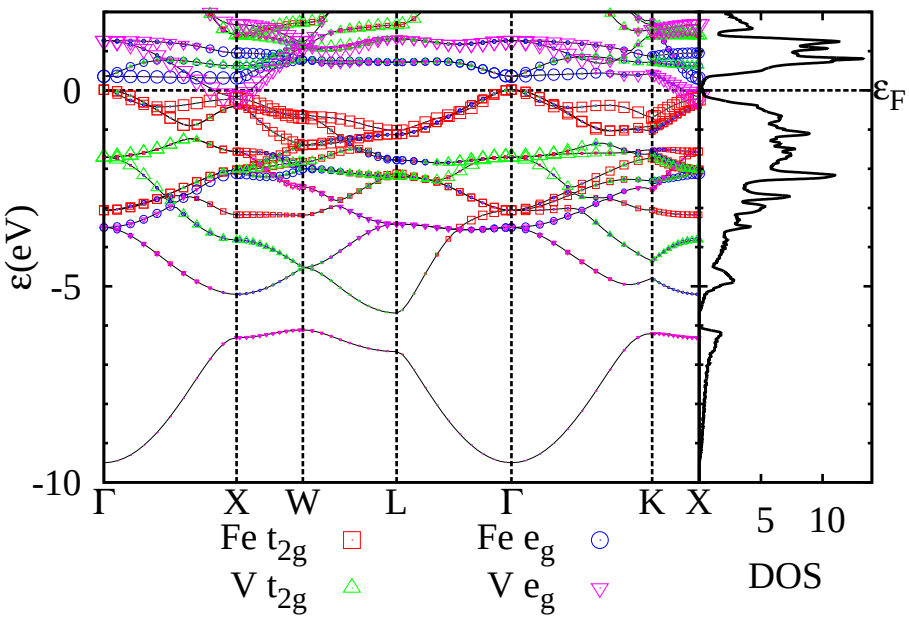

Figure 1 BD12028 11Aug2011

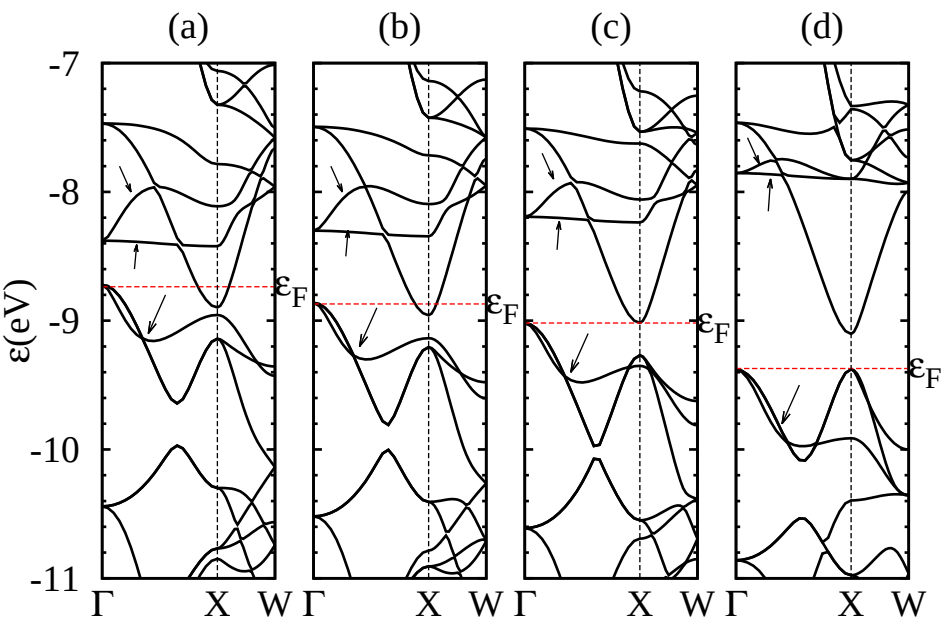

Figure 2 BD12028 11Aug2011

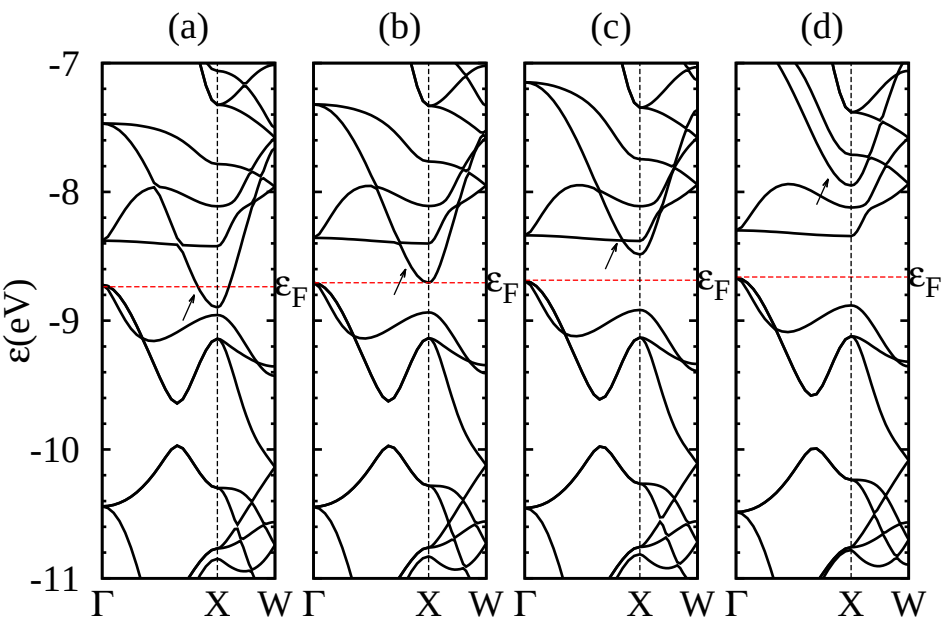

Figure 3 BD12028 11Aug2011

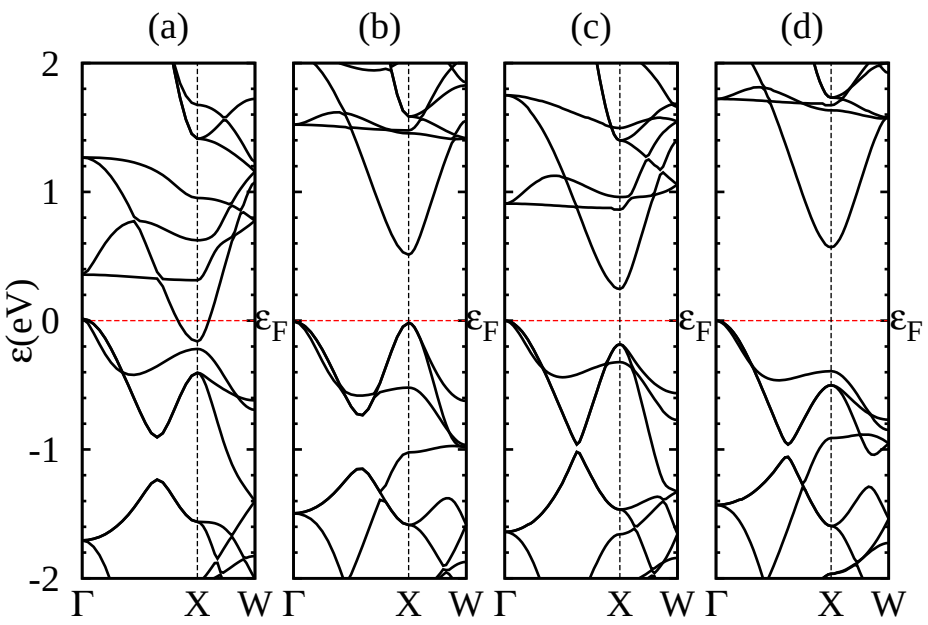

Figure 4 BD12028 11Aug2011

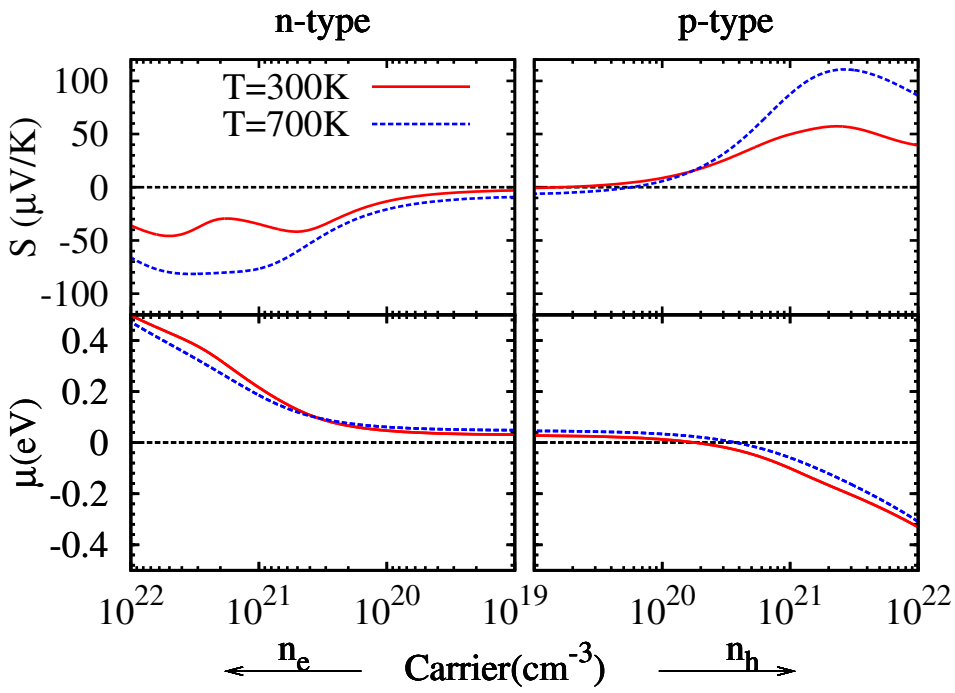

Figure 5 BD12028 11Aug2011

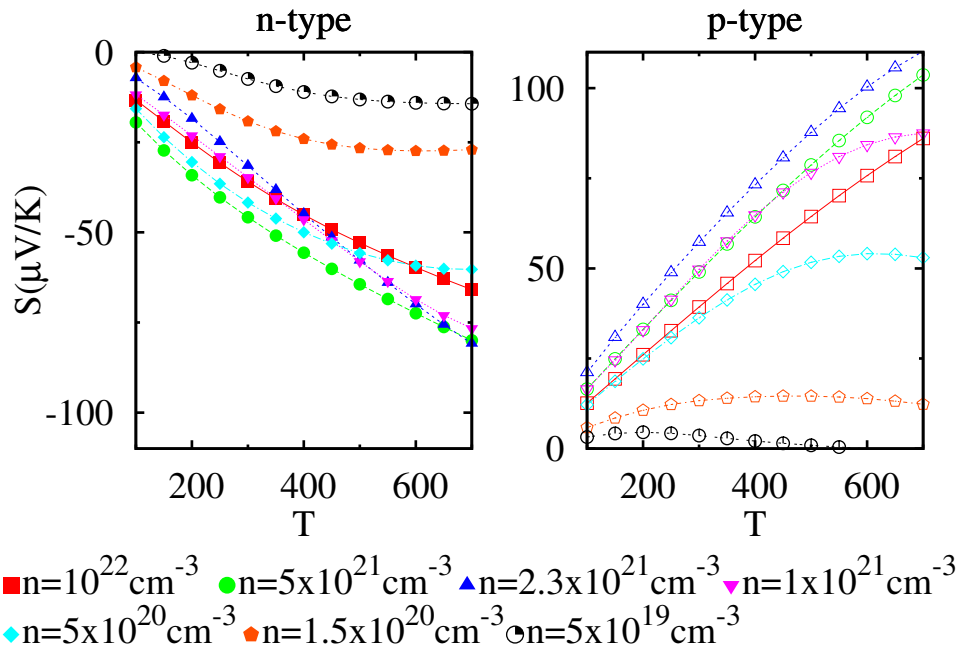

Figure 6 BD12028 11Aug2011

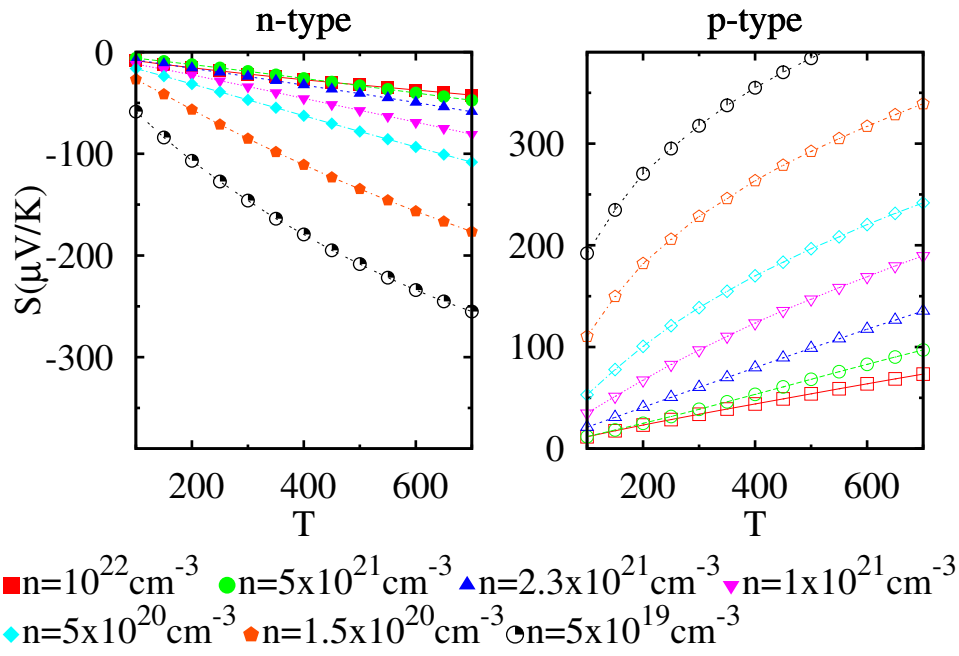

Figure 7 BD12028 11Aug2011

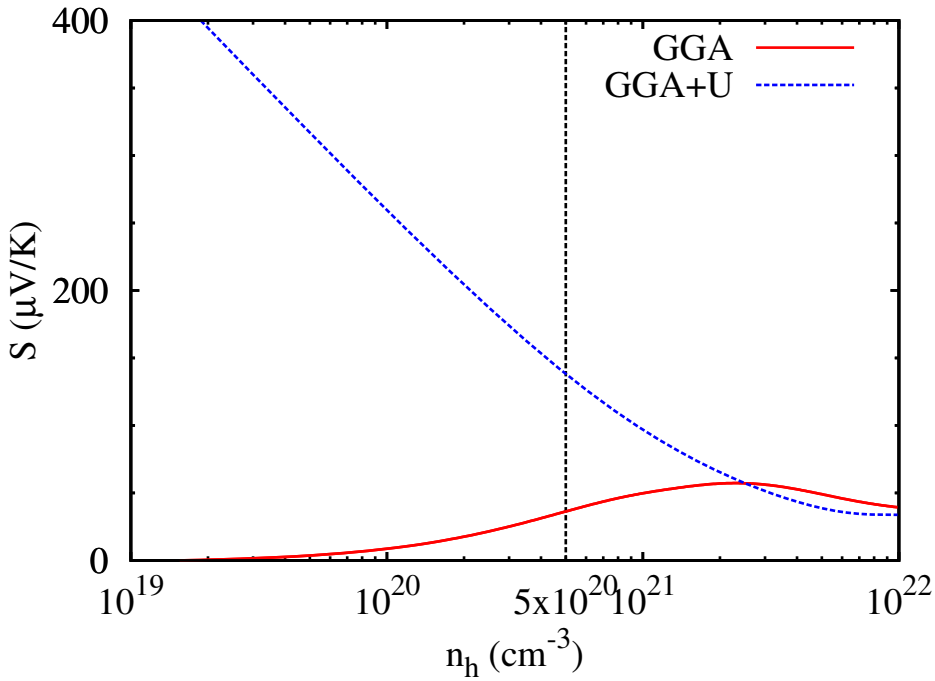

Figure 8 BD12028 11Aug2011

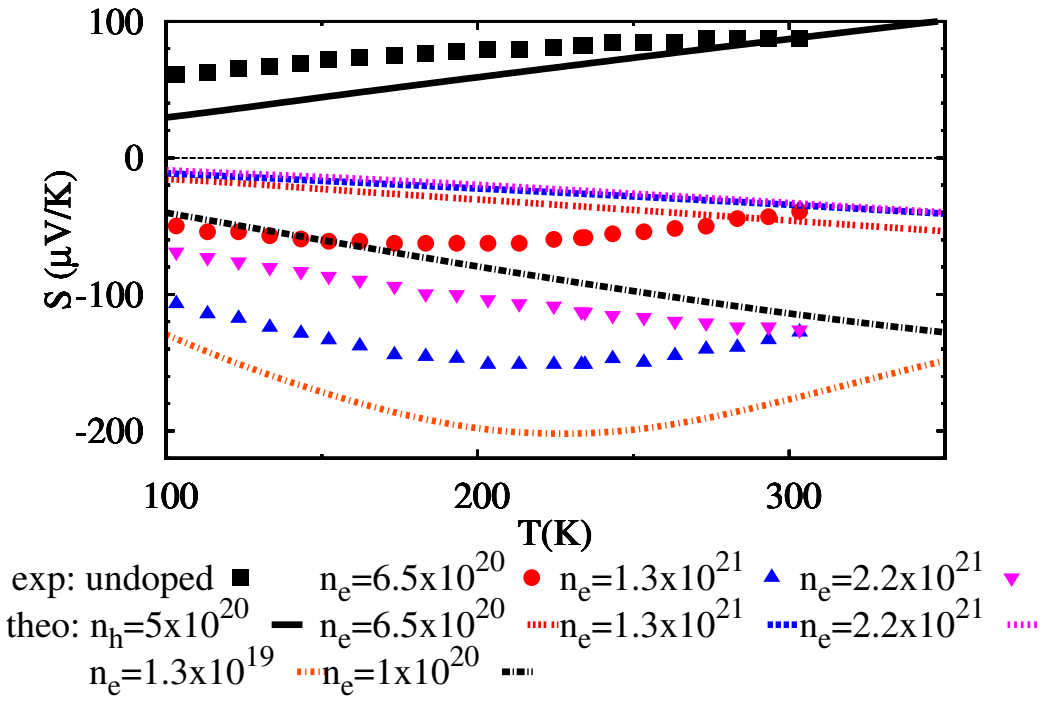

Figure 9 BD12028 11Aug2011